



**HAL**  
open science

## Assessing the capability of the SWAT model to simulate snow, snow melt and streamflow dynamics over an alpine watershed

Y. Grusson, X. Sun, Simon Gascoin, S. Raghavan, F. Anctil, Sabine Sauvage,  
J.M. Sánchez-Pérez

### ► To cite this version:

Y. Grusson, X. Sun, Simon Gascoin, S. Raghavan, F. Anctil, et al.. Assessing the capability of the SWAT model to simulate snow, snow melt and streamflow dynamics over an alpine watershed. *Journal of Hydrology*, 2015, 531, pp.574-588. 10.1016/j.jhydrol.2015.10.070 . hal-02351636

**HAL Id: hal-02351636**

**<https://hal.science/hal-02351636>**

Submitted on 11 Jun 2024

**HAL** is a multi-disciplinary open access archive for the deposit and dissemination of scientific research documents, whether they are published or not. The documents may come from teaching and research institutions in France or abroad, or from public or private research centers.

L'archive ouverte pluridisciplinaire **HAL**, est destinée au dépôt et à la diffusion de documents scientifiques de niveau recherche, publiés ou non, émanant des établissements d'enseignement et de recherche français ou étrangers, des laboratoires publics ou privés.

1        **Assessing the capability of the SWAT model to simulate**  
2        **snow, snow melt and streamflow dynamics over an alpine**  
3        **watershed**

4  
5  
6                    *Youen Grusson<sup>(a,f)</sup>, Xiaoling Sun<sup>(a,b)</sup>, Simon Gascoin<sup>(c)</sup>*

7        *Sabine Sauvage<sup>(a,b)</sup>, Srinivasan Raghavan<sup>(d)</sup>, François Anctil<sup>(f)</sup>, José Miguel Sanchez Pérez<sup>(a,b)</sup>*

8  
9        *<sup>a</sup> University of Toulouse; INPT, UPS; Laboratoire Ecologie Fonctionnelle et Environnement (EcoLab), Avenue*  
10                    *de l'Agrobiopole, 31326 Castanet Tolosan Cedex, France*

11                    *<sup>b</sup> CNRS, EcoLab, 31326 Castanet Tolosan Cedex, France*

12                    *<sup>c</sup> Centre d'Études Spatiales de la Biosphère (CESBIO), Toulouse, France*

13        *<sup>d</sup> Spatial Sciences Laboratory, 1500 Research Plaza, Office 221E, Texas A&M University, College Station, TX*  
14                    *77845*

15        *<sup>f</sup> Chaire de recherche EDS en prévisions et actions hydrologiques, Department of Civil and Water Engineering,*  
16                    *Université Laval, Québec, G1V 0A6, Canada*

17  
18        **contact:** youen.grusson.1@ulaval.ca ; Francois.Anctil@gci.ulaval.ca ; jose-miguel.sanchez-  
19        perez@univ-tlse3.fr

25 **Abstract:**

26

27 Snow is an important hydrological reservoir within the water cycle, particularly when the  
28 watershed includes a mountainous area. Modellers often overlook water stocked in snow pack  
29 and its influence on water distribution, especially when only some portions of the watershed is  
30 snow dominated. Snow is usually considered to improve hydrological modelling statistics, but  
31 without any regard for the realism of its representation or its influence on the hydrological cycle.  
32 This is all the more true when semi-distributed models are used, often considered inadequate  
33 for spatially representing such phenomena. On the other hand, semi-distributed models are  
34 being increasingly used to realise water budget assessment at a regional scale and such studies  
35 should not be realised without a good representation of the snow pack. Lack of field  
36 measurements is also a frequent justification for avoiding validating simulated snow packs. In  
37 this study, remote sensing data provided by MODIS is combined with *in situ* data, enabling the  
38 validation of the snow pack simulated by the Soil and Water Assessment Tool (SWAT), a semi-  
39 distributed, physically-based model, implemented over a partly snow-dominated watershed.  
40 Snow simulation was performed without complex algorithms or calibration procedures, using  
41 the elevation bands option included in the model and related snow parameters. Representation  
42 of snow cover and hydrological simulation were achieved by a standard automatic calibration  
43 of the model, over the 2000-2010 period, performed by SWAT-Cup/SUFI2, using six  
44 hydrological gauging stations along the fluvial continuum downstream of the snow-dominated  
45 area. Results highlight three important points: i) Set-up of elevation bands over mountainous  
46 headwater improved hydrological simulation performance, even well downstream of the snow-  
47 dominated area. ii) SWAT produced a good spatial and temporal representation of the snow  
48 cover, using MODIS data, despite a slight overestimation at the end of the snow season on the  
49 highest elevation bands. A comparison of the model estimate of snowpack water content with  
50 *in situ* data revealed an underestimation in water content in the lower part of the watershed and

51 a slight overestimation in its upper part. Those errors are linked and originate from difficulties  
52 of the model to incorporate very local spatial and temporal variations of the precipitation lapse  
53 rate. iii) Elevation bands brought consistent changes in water distribution within the  
54 hydrological cycle of implemented watersheds, which are more in line with expected flow  
55 paths.

56

57

58 **Keywords:** SWAT, MODIS, Hydrological modelling, Snow simulation, Elevation band,  
59 Garonne River.

60

## 61 **1. Introduction**

62

63 Water production is undeniably linked to mountainous areas that often contribute between 40 %  
64 and 60 % of global discharge, an estimation that can increase regionally up to 95 % (Viviroli  
65 and Weingartner, 1999; Viviroli et al., 2003). Therefore, in hydrological modelling, snowfall,  
66 snow accumulation, and snowmelt are among processes that have the greatest impact on the  
67 global water cycle. Differences in their estimation may cause substantial changes to  
68 hydrological simulations (Verbunt et al., 2003; Zeinivand and Smedt, 2009). This is all the more  
69 true when watersheds are located wholly or partly in mountains where, by temporarily storing  
70 water, snow affects the timing and amplitude of the seasonal hydrograph. Furthermore, many  
71 studies have highlighted the importance of taking snow processes into account when evaluating  
72 climate change impact (Barnett et al., 2005; Douville et al., 2002; Gurtz et al., 2005; Viviroli et  
73 al., 2011). Some models incorporate snow processes exclusively (Coughlan and Running, 1997;  
74 DeBeer and Pomeroy, 2009; Garen and Marks, 1996; Martelloni et al., 2012), using anything  
75 from a degree-day formulation to more complex energy budgeting to simulate snowmelt. From

76 an operational point of view, there are two main ways of accounting for snow in hydrological  
77 models. The most common method is to use the snow pack reservoir in the model only to  
78 improve performance on discharge simulation, without verifying the adequacy of the snow pack  
79 simulation in terms of water content, spatial distribution and temporal evolution (Troin and  
80 Caya, 2014; Wang and Melesse, 2005). The second method simulates snowpack conditions  
81 (Pradhanang et al., 2011) in order to obtain a good representation of the “snow water storage”  
82 as a part of the hydrological cycle. The latter approach is often constrained by the availability  
83 of *in situ* snow data with appropriate spatial and temporal resolutions. In this context, remote  
84 sensing is a valuable source of critical data. For instance, MODIS (Moderate Resolution  
85 Imaging Spectroradiometer) is one of the most used remotely-sensed snow data sources (Hall  
86 and Riggs, 2007; Klein and Barnett, 2003).

87

88 Regardless of whether validating snowpack or not in a model, studies concerned with the  
89 hydrological impact of snowmelt are often confined to watersheds immediately downstream of  
90 the principal snow accumulation areas – often small in size. Few studies have gone further by  
91 including downstream basins in their analysis. However, it is essential to take the influence of  
92 snow on the hydrological cycle into account, to improve water management on a larger scale,  
93 even if the watershed is not strictly snow dominated.

94

95 The Soil Water Assessment Tool (SWAT) model (Arnold et al., 1993) is a physically-based,  
96 comprehensive, continuous, semi-distributed and watershed-scale simulation model that allows  
97 the simulation of a large number of physical processes. It has been successfully implemented  
98 in many locations (Douglas-Mankin et al., 2010; Gassman et al., 2007). It includes a snow  
99 module, allowing the delimitation of up to ten elevation bands with associated temperature and  
100 precipitation lapse rates (Fontaine et al., 2002; Luo et al., 2012; Rahman et al., 2013).

101

102 In a previous study, Zhang et al. (2008) tested the benefits on SWAT discharge and runoff  
103 simulations to model snow without elevation bands, with elevation bands, and even with  
104 another more complex algorithm: SNOW17. Their results showed that using elevation bands is  
105 much more efficient than without. However, the use of a more complex algorithm failed to  
106 enhance discharge simulation and their conclusions were entirely based on hydrological  
107 performance and did not deal with the realism of snow representation.

108

109 The present study attempts to take the analysis further. It looks at determining how far SWAT  
110 is able to represent snow in terms of spatial and temporal distributions and stored water quantity.  
111 The analysis relies on a standard calibration procedure, i.e. based only on stream flow  
112 observations. No direct calibration of the snow pack or the snow water equivalent is realized,  
113 but these are assessed using MODIS and *in situ* data. Previous studies (Hong et al., 2010;  
114 Ouyang et al., 2010; Park et al., 2013; Stehr et al., 2009; Strauch and Volk, 2013) have  
115 experimented using MODIS data, but simply to validate SWAT streamflow simulations,. Only  
116 Stehr et al. (2009) have assessed the use of MODIS as a source of snow distribution data for  
117 validate SWAT snow simulations for a small, entirely snow-dominated basin, where no other  
118 data were available. The present study examines a much larger area than the Stehr et al. (2009)  
119 study (455 km<sup>2</sup>), focusing on the upper part of the Garonne River watershed (9200 km<sup>2</sup>), which  
120 drains a mountainous region. Another limitation of our study is the lack of reservoir  
121 management data to set up the SWAT model, a relatively common problem in hydrology, given  
122 the difficulties associated with obtaining such data from operators. The work presented here  
123 has thus been conducted without reservoir management data. The last part of the paper is  
124 dedicated to analysing how changes in snow dynamics representation influence SWAT water  
125 budget.

126

127 Several studies have been carried out in the investigated region. Fischer (1932); Pardé (1936);  
128 Probst (1983) provide comprehensive hydrological descriptions of the Garonne watershed.  
129 Voirin-Morel (2003) applied the hydrometeorological model ISBA-MODCOU, while Sauquet  
130 et al. (2010) used MODCOU and GR4J to simulate discharge over the Garonne river  
131 Watershed. Following from their work, Caballero et al. (2007) and Dupeyrat et al. (2008) tested  
132 the response of the Garonne River to climate change using CEQUEAU and ISBA-MODCOU.  
133  
134 Preliminary studies have also been performed using SWAT. Chea (2012) and Pinglot (2012)  
135 assessed pros and cons of using SWAT over this diversified catchment. They highlighted the  
136 important role played by snow accumulation and snow melt over the catchment. However, most  
137 SWAT applications on the Garonne focused on low altitude segments, deprived of the influence  
138 of snow (Boithias, 2012; Boithias et al., 2011; Ferrant et al., 2011; Oeurng et al., 2011).  
139  
140 Hence, the objectives of this study are: i) to explore the various snow representation  
141 possibilities, including elevation bands, offered by SWAT; ii) to validate SWAT snow  
142 simulations using MODIS data supplemented with *in situ* data; iii) to assess the impact of  
143 different snow dynamics computation on SWAT water budgets.

144

145

## 146 **2. Materials and methods**

### 147 **2.1. Study Area**

148 The Garonne River is 525 km long and one of the principal fluvial systems in France,  
149 draining a 55 000 km<sup>2</sup> area located in southwest France into the Atlantic Ocean. The large range  
150 of altitudes and slopes within the watershed leads to a diversity of hydrological behaviours that

151 could be attributed to three geographic entities: the Pyrenees to the south, the Massif Central to  
152 the north-east, and the plain between them (Probst, 1983).

153

154 The Pyrenean portion of the watershed largely influences the hydrological regime and consists  
155 of high mountains (some peaks exceed 3 000 m) above a large plain, whose elevation is less  
156 than a few hundred meters (Fig. 1). This portion, which represents nearly one sixth of the  
157 Garonne watershed and is largely influenced by topographic factors (Probst, 1983), is the focus  
158 of the present study. The Pyrenees portion of the Garonne river Watershed, which covers 9 200  
159 km<sup>2</sup>, has its outlet at Portet where an average flow of 189 m<sup>3</sup>/s (1910-2013) has been reported.  
160 The highest discharge on record reached 4,300 m<sup>3</sup>/s and the lowest was 23 m<sup>3</sup>/s. Over the same  
161 period, when looking at inter-annual mean monthly values, the highest flows occurs in May  
162 (348 m<sup>3</sup>/s) and the lowest in September (84 m<sup>3</sup>/s). Elevation ranges from 150 m to 3,145 m,  
163 while 44 % of the watershed has an elevation below 500 m and 20 % above 1,500 m. (Fig. 1).  
164 Land use analyses from Corine Land Cover maps (CLC, 2006) reveal that the plain is dominated  
165 by crops and pastures. Agricultural activities represent 49 % of the watershed, while the  
166 hillsides of the Pyrenees (35 % of the watershed) are covered by forests. For altitudes above  
167 2,500 m, vegetation is composed of alpine grassland and shrub.

168

169 According to the FAO soil classification on the European Soils Data Base map (ESDB, 2006),  
170 the soil composition is dominated by different types of cambisols (65 % of the catchment).  
171 Similar to the land use conditions, existing soil types differ with terrain condition and altitude.  
172 In the plain, calcic cambisol (27%) is dominating on eutric podzoluvisol (6%) orthic luvisol  
173 (6%) and fluvio-calcic fluvisoil (9%) that are present along streams. Slopes of the Pyrenees are  
174 dominated by dystic cambisols (32%) associated with orthic rendzina (5%). Above 2,500m,  
175 soil composition is divided between humic cambisols (5%), ranker (6%), and lithosols (3%).

176

177 Climate across the entire Garonne watershed does not reflect the same level of variability as for  
178 the Pyrenees. In the mountains, temperatures fall below freezing during winter months, while  
179 the winter temperatures in the plain generally remain positive. Dessens and Bücher (1997)  
180 stressed the variability of the Pyrenean precipitation, especially in winter when totals may be  
181 up to three times higher in the mountains than in the plain. In terms of temperature, analysis of  
182 Météo-France weather data provides a good example of this variability. Throughout the 2000-  
183 2010 period, mean minimum and maximum temperatures at the Genos station (1,250 m) in  
184 February were - 3°C and 3.5°C respectively. For the same period, the Blagnac station (151 m),  
185 only 120 km away, shows mean minimum and maximum temperatures of 3°C and 11.5°C (Fig.  
186 1). Variability in air temperatures associated with altitude the terrain causes irregularity in snow  
187 distribution: for instance the mountainous areas are snow dominated during winter while snow  
188 is absent in the plain all year long.

189

190 The watershed is also impacted by human activities, mainly by the presence of several dams  
191 obstructing the natural flow of the river. Subbasins 18, 24, 25, 26 and 27 (Fig.1) account for  
192 most of the reservoirs, which are primarily used for low flow support. Consequently, those  
193 reservoirs impact the hydrologic regime during the summer and the autumn but have a limited  
194 effect on the simulation of the snow processes. In Sauquet et al. (2010) and Hendrickx and  
195 Sauquet (2013), observed discharge data and naturalized discharge data are compared at four  
196 gauging stations : Valentine, Roquefort, Foix and Portet (Fig.1). This comparison highlights  
197 the limited impact of human activities on discharge during winter. Of the four gauging stations,  
198 only Foix seems to be partly impacted, over the January-March period. It should also be noted  
199 that this influence is not transmitted downstream to the Portet station.

200 **[Fig1 approximately here]**

## 201        **2.2.     *SWAT model***

202

203     SWAT was developed to simulate the impact of land use changes on hydrology, water quality  
204     and erosion. It is a semi-distributed model, based on a discretisation of the area. The first step  
205     of this discretisation consists in dividing the watershed into sub-watersheds, based on  
206     topography. SWAT then identifies hydrological response units (HRUs) within each sub-  
207     watershed, based on soil, land use, and slope. The HRUs are then used to compute a water  
208     balance based on four reservoirs: snow, soil, shallow aquifer, and deep aquifer. The main  
209     hydrological processes include infiltration, runoff, evapotranspiration, lateral flow, and  
210     percolation. Water balance computation is performed at the HRU level, aggregated at the  
211     subbasins level, and routed toward the reaches and the catchment outlet. The SWAT model has  
212     been chosen for this study because it has been successfully applied worldwide, over a wide  
213     range of scales, topographies, and climate conditions. It also allows the modeller to simulate  
214     various hydrological fluxes and reservoirs including snow (Douglas-Mankin et al., 2010;  
215     Gassman et al., 2007; Gassman et al., 2014). ArcSWAT 2012, which includes a GIS-based  
216     graphical interface, has been used for this study to define subwatersheds, HRUs and generate  
217     input files for the model.

218

219     For its water budget, SWAT distinguishes solid and liquid precipitation based on near-surface  
220     air temperature. The snowfall temperature parameter (SFTMP) is compared to the mean daily  
221     air temperature at subbasin scale; if it is lower than SFTMP, precipitation is then considered  
222     solid. If precipitation is considered solid, it is accumulated until snowmelt.

223

224     Snowmelt is mainly controlled by the air and snowpack temperature along with the daylight  
225     hours. Water volume generated by snowmelt process over a subwatershed, also depends on the

226 extent of the snow cover. Table 1 shows modifiable parameters related to snow at the catchment  
 227 level. A more comprehensive description of equations used by SWAT can be found in Neitsch  
 228 et al. (2011)

229  
 230

**Table 1: Modifiable snow parameters**

<b>SWAT parameters</b>	<b>Description</b>	<b>Default values</b>
<i>SFTMP</i>	Snowfall temperature	1.0°C
<i>SMTMP</i>	Snowmelt temperature	0.5°C
<i>SNO_SUB</i>	Initial snow water content	0 mmH <sub>2</sub> O
<i>SNOCOVMX</i>	Snow water content for 100 % snow cover	1.0 mmH <sub>2</sub> O
<i>SNOW50COV</i>	Fraction of SNOCOVMX corresponding to 50 % snow cover	0.5
<i>SMFMX</i>	Snow melt factor on 21 June	4.5 mmH <sub>2</sub> O/°C-day
<i>SMFMN</i>	Snow melt factor on 21 December	4.5 mmH <sub>2</sub> O/°C-day
<i>TIMP</i>	Snowpack temperature lag factor	1.0

231  
 232 In SWAT, snowfall, snowpack, and snowmelt processes are always computed by the model as  
 233 soon as the temperature falls below the threshold of snowfall temperature. But it also enables  
 234 those processes to be spatially refined as a function of elevation. A maximum of ten elevation  
 235 bands can thus be defined for subbasins as appropriate. Precipitation and temperature are then  
 236 taken into account for each individual elevation band, exploiting two lapse rates: one for  
 237 temperature (*tlaps* in °C/km) and one for precipitation (*plaps* in mm H<sub>2</sub>O/km/yr).

238  
 239 In this paper, the benefits of different snow computing and calibration options are tested. Three  
 240 different projects are set up: a first one, as a reference, without regard to snow calibration, a  
 241 second one using basin-scale global snow parameters, and a last one using elevation band  
 242 discretization and lapse rates. Table 2 and Figure 1 identify the seven subbasins where this last  
 243 variation has been implemented. (See section 2.4 for more details)

244  
 245 SWAT elevation bands (Fontaine et al., 2002) are set up by specifying their number, their mean  
 246 elevation, and the proportion of the subbasin area they encompass. However, there is no  
 247 consensus in the literature on a recommended number of elevation bands. Among the few  
 248 studies dealing with this issue, some define bands as a function of elevation (Fontaine et al.,

249 2002; Luo et al., 2012; Rahman et al., 2013; Stratton et al., 2009), while others define them as  
 250 a function of area (Pradhanang et al., 2011; Stehr et al., 2009; Zhang et al., 2008). The number  
 251 of bands varies from 1 to 10. Fontaine et al. (2002), who developed the snow module, found  
 252 that using 5 altitudinal bands improved simulation. As far as the authors are aware, only  
 253 Pradhanang et al. (2011) have compared simulations with various numbers of bands (0, 1, 3,  
 254 and 5). They concluded that using three or five elevation bands improved simulation. However,  
 255 the topography of their watershed was not as pronounced as for the Garonne: 800 m instead of  
 256 2,530 m (Table 2). Ten elevation bands were therefore set up here.

257  
 258 **Table 2: Statistics on elevation (m), including snow dominated subbasins (grey)**  
 259 (Locations are given in Fig.1)  
 260

Subbasin	Elevation				Subbasin	Elevation			
	Min	Max	Mean	Median		Min	Max	Mean	Median
1	140	276	203.9	212	15	195	1597	439.9	386
2	142	286	204.8	207	16	270	1566	499.9	441
3	143	200	163.0	162	17	198	1690	506.5	404
4	154	342	230.9	232	18	197	2317	526.2	400
5	178	362	257.7	260	19	420	2119	957.1	877
6	157	394	242.2	235	20	480	2136	1001.3	960
7	157	587	314.9	317	21	390	2826	1222.5	1117
8	155	798	313.2	287	22	377	2172	873.8	801
9	192	746	360.4	348	23	392	2840	1198.4	1116
10	265	503	315.0	297	24	419	3139	1485.2	1459
11	264	539	389.0	386	25	480	3146	1536.9	1517
12	319	567	384.8	368	26	471	3086	1702.6	1709
13	360	710	456.9	438	27	473	2886	1532.0	1555
14	322	2102	760.3	633	28	503	2928	1721.1	1775

261

### 262 **2.3. Model setup**

#### 263 **GIS layer and meteorological data sets**

264 Table 3 identifies the data sources used to set up the model. In order to delineate the watershed  
 265 and compute the flow directions of the river system, a digital elevation model (DEM) with a 90  
 266 m resolution from NASA and METI was employed (ASTER, 2011). Land uses come from the  
 267 Corine Land Cover (CLC, 2006) map on a scale of 1:100,000. The catchment is divided up into  
 268 25 land use types. Soil data are derived from the European Soil Database (ESDB, 2006) map

269 on a scale of 1:1,000,000, which relies on FAO soil classification adapted to SWAT by Chea  
 270 (2012). Climate data consist in daily time-step measurements from 12 Météo-France (French  
 271 weather forecasting agency) stations (Fig. 1), from January 1997 to December 2010.

272 **Table 3: Data sources**

Data type	Data source	Scale
DEM	NASA/METI (ASTER, 2011)	Grid cell 90m x 90m
Land use	Corine Land Cover (CLC, 2006)	1:100,000
Soil	European Soil Database (ESDB, 2006)	1:1,000,000
Climate	Météo-France ( <a href="https://donneespubliques.meteofrance.fr/">https://donneespubliques.meteofrance.fr/</a> )	
River discharge	Banque Hydro ( <a href="http://www.hydro.eaufrance.fr/">http://www.hydro.eaufrance.fr/</a> )	
Snow cover area	National Snow and Ice Data Center (NSIDC)	Grid cell 500m x 500m

273  
 274 **Hydrological data**

275 Monthly stream flow data from six selected gauging stations along the river continuum were  
 276 used to calibrate the model: Saint-Béat, Foix, Valentine, Roquefort, Auterive and Portet (Fig.1).  
 277 This selection was intended to represent the topographic diversity of the catchment – some are  
 278 located in the mountain range and others in the plain. Some of those stations are present on the  
 279 Garonne River (Saint-Béat, Valentine, Portet) while others are on its main tributaries: the Salat  
 280 (Roquefort) and the Ariège Rivers (Foix and Auterive). The aim was to perform a calibration  
 281 along the river continuum. Data originate from the *Banque Hydro* national database and cover  
 282 the period from 1997 to 2010. The only data missing over this period are: December 2008 for  
 283 the Valentine station and July to November 2000 for the Auterive station.

284  
 285 **Snow covers data: MODIS and *In situ* data**

286 Snow cover area data were extracted from the MOD10A2 product version 5 (Hall et al., 2006).  
 287 MOD10A2 provides syntheses of the maximum snow extent over a compositing period of eight  
 288 days from February 2000 to the present. For each pixel, MOD10A2 indicates whether snow  
 289 was detected at least once over a period of eight days (snow presence or absence). This product  
 290 is generated using observations from the Moderate Resolution Imaging Spectroradiometer  
 291 (MODIS) on board NASA's Terra satellite. The original grid spatial resolution is close to 500  
 292 m. The MOD10 series snow products have been extensively validated in various environments,

293 including mid-latitude mountainous areas (Hall and Riggs, 2007). MOD10A2 is well suited to  
294 hydrological studies because most of the cloud-covered pixels are eliminated by the  
295 compositing procedure (Magand et al., 2013). However, cloud-covered pixels will remain in  
296 the MOD10A2 synthesis whenever clouds persist more than eight days. Missing data have been  
297 interpolated in order to allow a direct comparison with the model output as described in  
298 (Gascoin et al., 2015).

299

300 MOD10A2 tiles over the Pyrenees were first assembled and reprojected in the Lambert-93  
301 reference system at 500 m resolution using the nearest-neighbour option in the MODIS  
302 Reprojection Tool (Dwyer and Schmidt, 2006). A simple gap-filling algorithm adapted from  
303 Parajka and Blöschl (2008) was then applied to interpolate the remaining pixels obstructed by  
304 clouds. The algorithm works in three sequential steps: (i) spatial filter: each cloud pixel is  
305 reclassified as snow (no snow) if at least five of the eight adjacent pixels are classified as snow  
306 (no snow); (ii) temporal filter: a cloud pixel is reclassified as snow (no snow) if the same pixel  
307 is classified as snow in both the preceding and the following grid (*i.e.* in the previous and the  
308 subsequent eight-day syntheses). This temporal filter can be extended to the grids  $n+2$  and/or  
309  $n-2$  if cloud obstruction persists in grids  $n+1$  and/or  $n-1$ ; (iii) the remaining cloud-covered pixels  
310 are reclassified on an image basis using a classification tree taking into account four prediction  
311 variables derived from the location and the topography (pixel elevation, aspect, northing and  
312 easting). The resulting gap-free product was extracted from the seven snow-dominated  
313 subbasins of the study area (Tab. 2) to compute the snow cover area time series at the eight-day  
314 time step. However, MOD10A2 data before gap-filling were used for the spatial comparison  
315 with the model results (see point 3.1).

316

317 Manual snowpack measurements from six Météo-France sites (Fig.1) are available from 2000  
318 to 2010 at a daily time step (<https://donneespubliques.meteofrance.fr/>). They are spread across

319 subbasins 23, 24, and 25. Two monitoring stations at different elevations are present in each of  
 320 those subbasins. Table 4 provides details of their elevation, location, affiliated subbasin and  
 321 elevation band numbers.

322  
 323

**Table 4 : Snow monitoring information**

Station name	Elevation(m)	Lat	Long	Subbasin	Band
Aulus les Bains	733	42°48'N	1°20'E	23	2
Port d'Aulas Nivose	2140	42°46'N	1°07'E	23	8
St Lary Soulan	827	42°49'N	0°19'E	24	2
Eget	1016	42°47'N	0°16'E	24	3
St Paul d'Oueil	1115	42°50'N	0°33'E	25	3
Maupas-Nivose	2430	42°43'N	0°33'E	25	8

324  
 325

## 326 **2.4. Model sensitivity analysis and calibration**

327 Model sensitivity analysis and calibration were performed for three SWAT projects. The  
 328 *reference project* uses standard parameters and default values for the snow parameters (and no  
 329 elevation bands). These parameters are then passed to the following two projects. The *snow*  
 330 *parameters project*, as suggested by its name, identifies the snow parameters but not the  
 331 elevation band parameters. Finally, the *elevation bands project* adds ten elevation bands to the  
 332 snow-dominated subbasins.

333 Sensitivity analysis and calibration were undertaken by SWAT-Cup (Abbaspour, 2013), and its  
 334 SUFI-2 algorithm (Abbaspour et al., 2004). SWAT-Cup is an external software tool allowing  
 335 SWAT users to realise automatic calibration with more comfort and efficiency, which has been  
 336 used increasingly by the SWAT community (Arnold et al., 2012). In SWAT-Cup, users have  
 337 the option between different calibration algorithms of which SUFI-2 is known to achieve a good  
 338 calibration performance in a limited number of iterations (Yang et al., 2008).

339 A large number of parameters may be calibrated through SWAT-Cup, making SWAT a very  
 340 adaptive model. Only a subset of them may actually be selected for a sensitivity analysis. In  
 341 this study, the initial parameter selection was interpreted on previous SWAT modelling across

342 the Pyrenees and the Garonne watershed (Boithias, 2012; Chea, 2012; Oeurng et al., 2011;  
 343 Pinglot, 2012).

344

345 The sensitivity analysis methodology follows the one-at-a-time procedure proposed in  
 346 Abbaspour (2013). This procedure tests SWAT sensitivity to changes in a parameter, when all  
 347 other parameters are kept constant. Sampling relies on the latin hypercube method (McKay et  
 348 al., 1979) in order to cover all the domain of variation of the parameters, dividing the user-  
 349 defined ranges into several subranges of equal probability. In all, 32 parameters were  
 350 considered (Table 5): 21 hydrological parameters for the reference project, 8 for the snow  
 351 parameters project and 3 for the elevation bands project. Five runs were performed over the ten-  
 352 year period from 2000 to 2010, preceded by a three-year warming period (1997-2000).

353

354

**Table 5: Parameters considered for the sensitivity analysis**

Parameters	Description	Min	Max	Default
<b><u>HYDOLOGICAL PARAMETERS</u></b>				
EPCO	Plant uptake compensation factor	1	0	1
SURLAG	Surface runoff lag time	0.5	1	4
GW_Delay	Groundwater delay	0	500	31
GW_Revap	Groundwater "revap" coefficient.	0.02	0.2	0.02
GWQMN	Threshold in the shallow aquifer for return flow to occur	0	5000	1000
GWHT	Initial groundwater height	0	25	1
GW_SPYLD	Specific yield of the shallow aquifer	0	0.4	0.003
SHALLST	Initial depth of water in the shallow aquifer	0	50000	500
DEEPST	Initial depth of water in the deep aquifer	0	50000	1000
ALPHA_BF	Base flow alpha factor (days)	0	1	0.048
REVAPMN	Threshold in the shallow aquifer for "revap" to occur	0	500	0
RCHRG_DP	Deep aquifer percolation fraction	0	1	0.05
ESCO	Soil evaporation compensation factor	0	1	0.95
CN2 (relative test)	SCS runoff curve number	-0.2	0.2	HRU
CANMX	Maximum canopy storage	0	100	HRU
OV_N	Manning's "n" value for overland flow	0.01	30	HRU
SOL_AWC (relative test)	Available water capacity of the soil layer	-0.5	0.5	soil layer
SOL_K (relative test)	Saturated hydraulic conductivity	-10	10	soil layer
SOL_Z (relative test)	Depth from soil surface to bottom of layer	-500	500	soil layer
EVRCH	Reach evaporation adjustment factor	0.5	1	1
EVLAI	LAI at which no evaporation occurs from water surface	0	10	3
<b><u>SNOW PARAMETERS</u></b>				
SFTMP	Snowfall temperature	-10	10	4.5
SMTMP	Snowmelt base temperature	-10	10	4.5
TIMP	Snowpack temperature lag factor	0	1	1
SMFMX	Maximum melt rate for snow during year (summer solstice)	0	20	1
SMFMN	Minimum melt rate for snow during year (winter solstice)	0	20	0.5
SNOW50COV	Snow water equivalent that corresponds to 50% snow cover	0	1	0.5
SNOWCOVMX	Snow water content that corresponds to 100% snow cover	0	100	1
SNO_SUB	Initial snow water content	0	300	0
<b><u>ELEVATION BAND PARAMETERS</u></b>				
TLAPS	Temperature lapse rate	-10	10	-6
PLAPS	Precipitation lapse rate	-100	500	0
SNOEB	Initial snow water content in elevation bands	0	300	0

355

356 Once sensitive parameters have been identified, a 1500-run calibrations, as recommended in  
357 Yang et al. (2008), were performed three time (one for each project), for the six gauging stations  
358 identified in Figure 1. SWAT-Cup allows the user to select subbasins for calibration. In order  
359 to avoid possible conflict caused by the use of hydrologically-connected gauging stations, three  
360 groups of subbasins were created. Parameters were thus identified in three steps from upstream  
361 to downstream, leading to different values for each group. Group 1 included subbasins upstream  
362 of Saint-Béat, Roquefort and Foix; Group 2 included the remaining subbasins upstream of  
363 Portet: Valentine and Auterive; Group 3 is the outlet of the catchment: Portet. Snow parameters  
364 for the other two projects were identified in a second step, but at catchment scale, using all six  
365 gauging stations simultaneously. Elevation band parameters were finally identified, at subbasin  
366 scale, for snow-dominated subbasins (Table 2), using all six gauging stations simultaneously.  
367 Calibration and performance criterion calculations have been performed without regard to  
368 missing data, as allowed by SWAT-Cup. For each gauging station, calibration was conducted  
369 using the Nash-Sutcliffe criterion (NS) (Nash and Sutcliffe, 1970) as the objective function.  
370 This metric is normalized in order to allow comparing between the variance of the observed  
371 dataset and the existing residual variance between this same observed dataset and the simulated  
372 one. NS ranges from  $-\infty$  to 1 and is sensitive to large errors. The NS equals 0 when the model  
373 is as accurate as the mean of the observed data set and NS equals 1 when the model offers a  
374 perfect fit. After calibration, performance was also evaluated based on the percent bias (Pbias).  
375 This second metric measures the average bias existing between simulated and observed data. It  
376 is given as a percentage. A negative value indicates underestimation while a positive value  
377 indicates overestimation. Bias is nil when Pbias equals 0.

## 378 **2.5. Validation of snow simulation**

379

380 MODIS and *in situ* data are only used for validation. Neither of them can be used for calibration.  
381 SWAT computes snow water equivalence – discretised or not by elevation band – when MODIS  
382 detects the presence of snow in term of surface and *in situ data* would have required a very  
383 dense spatial density for calibration, which is not available.

384

385 After calibration, MODIS and the observed snow data were used to validate SWAT snow  
386 simulation. Simulated spatial and temporal series were compared to MODIS data and temporal  
387 series to *in situ* snowpack observations.

388 Spatial analysis compares snow presence and absence for specific days: during the maximum  
389 extent of the snow period and at the end of the snow period, when the snow is melting and its  
390 extent reduced, *i.e.* around mid-February for the maximum extent and in May for the end of the  
391 melting period. The MODIS detection level was estimated to be about 15 mm of snow water  
392 equivalent (SWE) following Klein and Barnett (2003). Accordingly, the presence of snow in  
393 SWAT maps was confirmed only for simulated SWE above 15 mm, based on the average value  
394 for all HRUs present per elevation band.

395

396 Temporal analysis was performed on each snow-dominated subbasin, comparing SWE in two  
397 different ways: MODIS and manual observations. For MODIS, the validation was undertaken  
398 at subbasin scale, by averaging daily SWE values of all bands on every subbasin over the entire  
399 simulation period. For the *in situ* observation, validation was performed at the station scale.  
400 Since only the snowpack depth was actually measured, snowpack densities between 0.2 and  
401 0.45, typical of the Pyrenees (Fassnacht et al., 2010; Lopez-Moreno et al., 2013), were explored  
402 to allow a comparison of SWE and SWAT outputs.

403

404 **3. Results**

405 **3.1. Model performance**

406 The sensitivity analysis identified the most influential parameters for each project (Table 6)  
 407 from the initial list given in Table 5. Ten of the twenty-one hydrological parameters influence  
 408 the variance of the first SWAT project, while the majority of the snow and elevation band  
 409 parameters are also retained for the same reasons.

410

411

412

**Table 6: Influential parameters**

Hydrological parameters		Snow parameters		Elevation band parameters
GW_Delay	RCHRG_DP	SMFMX	SMTMP	TLAPS
GW_Revap	ESCO	SMFMN	TIMP	PLAPS
GWQMN	CN2	SNOW50COV		
ALPHA_BF	CANMX	SNOWCOVMX		
REVAPMN	SOL_AWC	SFTMP		

413

414

415 Calibrated values for each group of subbasins created for the abovementioned reasons are

416 presented in Table 7.

417

418

**Table 7: Calibrated values for each project**

<i>Reference project</i>				
Parameters	Calibration Range	Calibrated values		
		Group 1	Group 2	Group 3
CN2.mgt (Relative from HRU values)	-0.1/+0.01	+0.065	-0.020	-0.06
SOL_AWC.sol (Relative from Soils layers values)	-0.05/+0.05	-0.038	-0.042	-0.004
GW_DELAY.gw (Relative from default values=31)	-30/60	4.63	87.19	22.15
GWQMN.gw (Relative from default values=1000)	-500/500	1033.67	806.33	679.00
GW_REVAP.gw	0.02/0.2	0.10	0.12	0.03
RCHRG_DP.gw (Relative from default values=0.05)	-0.04/0.04	0.04	0.05	0.04
ALPHA_BF.gw	0/1	0.23	0.25	0.75
REVAPMN.gw	0/1000	467.00	449.67	583.00
CANMX.hru	0/30	16.81	19.57	0.39
ESCO.hru	0.5/0.95	0.56	0.80	0.85
<i>Snow parameters project</i>				
Parameters	Calibration Range	Calibrated values		
		Subbasins calibrated: All (catchment scale)		
SFTMP.bsn	-2/2	1.30		
SMTMP.bsn	-2/2	1.97		
SMFMX.bsn	2/6	4.96		
SMFMN.bsn	2/6	3.16		
TIMP.bsn	0/1	0.14		
SNOCOVMX.bsn	0/50	38.38		
SNO50COV.bsn	0.3/0.7	0.50		
<i>Elevation bands project</i>				
Parameters	Calibration Range	Calibrated values		
		Subbasins calibrated		Snow dominated subbasins
		All (catchment scale)		

SFTMP.bsn	-2/2	1.52	
SMTMP.bsn	-2/2	-0.49	
SMFMX.bsn	2/6	3.05	
SMFMN.bsn	2/6	5.84	
TIMP.bsn	0/1	0.54	
SNOCOVMX.bsn	0/50	29.48	
SNO50COV.bsn	0.3/0.7	0.64	
TLAPS.sub (Relative from default values=-6)	-2/2		-0.61 (= -6.61)
PLAPS.sub (Relative from default values=200)	-100/500		+423.40 (= 623.40)

419

420

421 The results associated with each project are illustrated in Table 8. The performance of the

422 *reference project* is poor overall: the mean NS criterion for monthly discharge reaches only

423 0.22, while Pbias is 24.5%. Only one gauging station has NS higher than 0.5. Retaining those

424 calibrated hydrological parameters and identifying snow parameters (snow parameters project)

425 worsened performance: a mean NS of 0.15 and Pbias of 39.83%. Even though NS improved at

426 the final outlet (Portet), seeking snow parameters that are valid for all mountainous elevations

427 proved to be difficult, if not impossible. Indeed, results for some stations are improved

428 (Valentine, Portet) while others are worse (Roquefort, Auterive), creating inconsistency in

429 performance at catchment scale. Pbias followed a similar trend, since only Valentine and Portet

430 improved compared with the reference project. On the other hand, the elevation bands project

431 led to a better performance: mean NS of 0.53 and Pbias of 3.98. Performances in terms of NS

432 are now more consistent with the ones in the reference project. Except for Valentine, all gauging

433 stations improved in performance. It is also noteworthy that the improvement is not only limited

434 to the snow-dominated subbasins, but is also transmitted down to the outlet of the catchment

435 (Portet), located tens of kilometres into the plain and where the largest gain in realised: NS of

436 0.88 instead of 0.21 and Pbias of 1 instead of 47.3.

437

438 **Table 8 : Calibration performance: NS and P-bias for each gauging station at a monthly time step and for**  
439 *each calibration project: reference, snow parameters and elevation bands projects*

440

	<i>Reference Project</i>		<i>Snow parameters Project</i>		<i>Elevation bands project</i>	
	NS	P-Bias (%)	NS	P-Bias (%)	NS	P-Bias (%)
<b>Saint Béat</b>	0.18	4.4	0.24	22.3	0.48	-15.1
<b>Foix</b>	0.14	37.4	-0.16	56.5	0.61	25.7
<b>Roquefort</b>	0.67	16.7	-0.03	57.8	0.69	0.2
<b>Valentine</b>	0.3	-15	0.75	1.4	0.28	-34.2

<b>Auterive</b>	-0.17	56.2	-0.46	66.5	0.18	46.3
<b>Portet</b>	0.21	47.3	0.57	34.5	0.88	1

441

442

### **3.2. Snow simulation**

443

Streamflow simulation is improved introducing elevation bands to the model setup. This study

444

tries to go further by considering the temporal evolution of the simulated snow cover. The latter

445

was assessed comparing SWAT outputs to MODIS data at 10 February 2005, which roughly

446

corresponds to the maximum snow cover (Figure 2-A), and at 10 May 2005, which is typical

447

of the end of the snow season (Figure 3-B).

448

449

SWAT snow cover in Figure 2-A is fairly consistent with MODIS data, especially for subbasins

450

21 and 26. It is somehow underestimated in subbasins 27, 24, and 25 and overestimated in

451

subbasin 23 where the largest disparity is noticed. On the other hand, SWAT melting lags

452

MODIS data in Figure 2-B, but snow is then limited to the mountain tops. Overall

453

representation of snow in Figure 2-B is slightly overestimated by SWAT. Subbasins 27 and 24,

454

where snow is underestimated during snow season, improve during the melting period.

455

456

**[Fig2 approximately here]**

457

458

The previous analysis was complemented by a time-series comparison of the MODIS

459

percentage of snow cover and SWAT snow water equivalent for the entire ten-year period.

460

Figure 3 illustrates the extent of snow cover period. The MODIS data depict the surface area

461

covered by snow, while SWAT provides snow water equivalent values. For most years and

462

subbasins, SWAT and MODIS snow season begins simultaneously, even if a delay is noticeable

463

for SWAT in 2005 or 2007 and for some subbasins in 2006. There is less agreement at the end

464 of the snowmelt period, when SWAT maintains snow longer than that reported by MODIS data,  
465 as in Figure 2. The peak of the snowpack also occurs later for SWAT than for MODIS.

466

467 **[Fig3 approximately here]**

468

469 A comparison was also carried out between SWAT snow water equivalent and a range of snow  
470 water equivalent values calculated from the snowpack depth time series (2000-2010). However,  
471 for the sake of clarity, the analysis presented here focused on the 2004-2005 snow accumulation  
472 and melting periods, which offered the widest spatial coverage – in practice, only the *Maupas-*  
473 *Nivose* site is affected by missing data, so 2003-2004 is used at that site instead. As a first step,  
474 Figure 4 compares SWAT snow outputs for the elevation bands to which the stations belong,  
475 and to the upper or lower bands for completeness.

476

477 **[Fig4 approximately here]**

478 The comparison reveals the altitudinal distribution of the snow water equivalent within SWAT.  
479 Simulations for the highest sites, Port d’Aulus Nivose and Maupas Nivose (elevation band 8),  
480 overestimate the snowpack while lower elevation bands offer a closer fit to the observations.  
481 The same discrepancy occurs for the lower stations (Aulus-les-Bain, Saint Larry Soulan, Eget,  
482 Saint Paul d’Oueil) where higher bands offer a better agreement to the observations. These  
483 findings are consistent with the previous spatial and temporal analyses.

484

## 485 **4. Discussion**

### 486 **4.1. Model sensitivity analysis and calibration**

487

488 Parameters deemed influential by the sensitivity analysis are consistent with those of other  
489 studies, particularly Stratton et al. (2009) where sensitivity is explored in the context of water  
490 budget under snow influence. The two main differences concern ground water delay and  
491 maximum canopy storage. Ground water delay (GW\_DELAY) is lower in the upper part of the  
492 catchment because of its altitudinal soil structure and slope that favour water circulating faster  
493 than in the plain. The presence of a dam upstream of the Valentine gauging station may also  
494 provide an explanation. For the same reason, canopy storage (CANMAX) differs since the  
495 upper part is mostly forested and the lower parts foster agricultural grassland and fields.

496 Important similarities between parameters considered as sensitive can also be observed in  
497 Palazón and Navas (2014). In this work, conducted over a proximal watershed on the Spanish  
498 side of the Pyrenees, sensitive parameters related to groundwater circulation and snow are  
499 identical. The only difference is this initial volume of water in the aquifers, which are not  
500 considered sensitive in our case, as regard of the 3 years warmup period performed.

501  
502 Only two elevation band parameters are non-influential: the initial water content parameters  
503 SNO\_SUB and SNOEB. Insensitivity may originate from using a three-year warming period,  
504 which diminishes their influence on the variance of the model outputs by balancing this  
505 reservoir before the first year of simulation. Differences between the *snow parameters project*  
506 and *elevation bands project* culminate in the snowpack lag factor (TIMP) and snow melt  
507 temperature (SMTMP). In the *snow parameters project*, SMTMP appeared slightly too high  
508 (1.97 °C), but the use of elevation bands reduced it to a more likely value (-0.49 °C). PLAPS  
509 and TLAPS calibrated value are consistent with values used by Palazón and Navas (2014)  
510 where TLAPS values is set to -5.0C°/km and PLAPS is set to values between 550 and 1000  
511 mm/km depending on the watershed considered.

512

513 The performance of the reference project stresses the possible drawbacks of calibrating a project  
514 when only the upper part of the catchment is snow dominated. Improving the simulation  
515 identifying snow parameters at basin scale is not very effective either. However, identification  
516 of the elevation band parameters clearly improved the performance, not only for the snow-  
517 dominated subbasins, but also for the plain downstream.

518

## 519 **4.2. Validation of snow simulation**

520

521 SWAT elevation bands improve hydrological performance and lead to plausible snowpack  
522 simulations. Highlights of some elements of the analysis are summarized below:

523 First, comparison of snow simulations, with *in situ* data revealed a non-homogeneous error:  
524 snow is overestimated in higher elevations and underestimated in lower ones. The fact that  
525 the error is not a function of altitude impedes any improvement based on linear temperature  
526 or precipitation lapse rates alone. As underlined by many authors, *e.g.* Kirchner et al. (2013)  
527 and Minder et al. (2010), orogenic lapse rate is a complex phenomenon, highly dependent  
528 on local topographic factors, such as valley shapes, seasonal variations, and temporal  
529 phenomena such as temperature inversion and foehn wind. Rijckborst (1967) analysed  
530 precipitation measurements over the upper part of the Garonne – corresponding to subbasin  
531 28 in Fig1 – and found lapse rate from 340 to 880 mm/km/year. Castellani (1986) in northern  
532 Alps, founds that area judged as homogeneous in terms of precipitation, lapse rates from 200  
533 to 600 mm/km/yr. Hence, the identification of a single temperature and precipitation lapse  
534 rates over large watersheds will inevitably lead to errors. Winter temperature inversion is  
535 also a common phenomenon across the Pyrenean area (Pagès and Miró, 2010; Pepin and  
536 Kidd, 2006). It could lead to a reduction in snowfall uphill and an increase downhill, which  
537 is consistent with the SWAT snowpack simulation error.

538 Second, a consequence of the overestimation in higher elevations, the snow cover area near  
539 the end of the melting period and the snowmelt duration are also overestimated. However,  
540 SWAT could only compute snow on each elevation band – a finite entity – which is  
541 restrictive. Elevation bands represent, in some way, the maximum spatial resolution of the  
542 model. Snow in the higher parts of subbasins is definitely a sensitive part of the computation  
543 process, which specifically could require more resolution. On the basis of that assessment,  
544 two options appear feasible: modify the SWAT model to compute more bands, thereby  
545 increasing the model resolution, or use the ten bands already available differently, by not  
546 setting them up regularly from top to bottom, but with thinner bands in the upper part.  
547 However, the present study deals with bands that are set up using an equal elevation fraction  
548 (10 %) and does not test snow simulation driven by computation using bands of an equal  
549 area fraction. By using irregularly spaced elevation bands with thinner bands at higher  
550 altitudes, covering a smallest surface and elevation range, resolution in the higher elevation  
551 will be increased. As SWAT uses the mean elevation in each band to compute the change in  
552 temperature and precipitation, the increased elevation range represented by upper bands  
553 could reduce the overestimation observed in the present study. Weather data are also  
554 essential parameters in the snow simulation process. This study was developed using 12  
555 different weather stations (Figure 1), which is a substantial number for this 9,200 km<sup>2</sup>  
556 catchment in comparison to other successful studies (Bieger et al., 2014; Stehr et al., 2009).  
557 Moreover, data from each station can be considered reliable, with the mean rate of missing  
558 values over the simulated period being 0.25 % for temperature data and 0.5% for  
559 precipitation data.

560 Finally, scarcity of reservoir management data doesn't seem to be determining in the snow  
561 dynamics simulation, even after calibration process. When comparing subbasins affected by  
562 reservoir management, particularly for subbasin 26 and 27, which were found to be the most  
563 impacted during winter (Sauquet et al., 2010), and non-impacted subwatershed (21, 23, and

564 28), no substantial difference can be detected between snow simulation error time series,  
 565 after validation with the MODIS data.

566

567 **4.3. Impact on the hydrological cycle**

568

569 Modifications in snow dynamics will drive changes in SWAT water partitioning at subbasin  
 570 scales.

571 Introduction of elevation bands and their associated parameters, such as the precipitation lapse  
 572 rate, change the estimated volume of precipitation received by each subbasin. Table 9 highlights  
 573 this variation from one SWAT project to the others. Changes are substantial for subbasins 27  
 574 and 21 in which the increase of annual precipitation volume is more than 50% - note than both  
 575 subbasins underestimated the mean annual precipitation when simulated without elevation  
 576 bands. This may result from the use of a unique weather data for the entire subbasins and from  
 577 station site elevation much closer to the valley than to the mountain peaks. For instance,  
 578 subbasin 21 relies only on the St Giron weather station (elevation of 414 m) when the subbasin  
 579 elevation varies from 390 to 2826 m, leading to a possibly wrong total precipitation. On the  
 580 other hand, precipitation lapse rates were calibrated here from seven snow-dominated subbasins  
 581 and may not be pertinent for neighbour subbasins. This is likely the case for subbasin 23 where  
 582 an overestimation of snow cover extent has been detected.

583

584 **Table 9: Mean Annual precipitations (mm/year) for hydrologic years (from September to August)**  
 585 **over 2000-2010 for each snow dominated subwatershed.**

586

*A=Reference project; B = Snow parameters project; C = Elevation bands project.*

Subwatersheds	28	27	26	25	24	23	21
A / B	1558	876	1625	1558	1558	1625	918
C	1845	1372	2292	1904	1885	2188	1528
Var %	+18	+57	+41	+22	+21	+35	+66

587

588 The presence or absence of snow cover will also strongly affect the water balance. Therefore,  
589 it differs from one project to the others, especially runoff, infiltration and actual  
590 evapotranspiration (AET), allowing more water to be stored in the watershed as snow and soil  
591 moisture. Table 10 illustrates differences in the annual water partitioning for each subbasin.  
592 AET is the main water flux before introduction of elevation bands on the model set up. When  
593 using elevation bands, fraction of annually evapotranspirated water decrease. Infiltration then  
594 becomes the main water flux along with runoff.

595  
596  
597

**Table 10 : Water partitioning within snow-dominated subbasins.**  
*Mean Annual data over 2000-2010 (hydrologic years from September to August).*

Subwatershed		28	27	26	25	24	23	21	
<i>Reference Project</i>	<b>Precipitation</b>	<b>mm</b>	<b>1558</b>	<b>876</b>	<b>1625</b>	<b>1558</b>	<b>1558</b>	<b>1625</b>	<b>918</b>
	Evapotranspiration	mm	822	662	878	813	792	982	817
		%	53	76	54	52	51	60	89
	Runoff	mm	346	66	338	192	318	169	62
		%	22	8	21	12	20	10	7
	Infiltration	mm	389	148	408	552	448	474	39
		%	25	17	25	35	29	29	4
	<i>Snow parameters project</i>	<b>Precipitation</b>	<b>mm</b>	<b>1558</b>	<b>876</b>	<b>1625</b>	<b>1558</b>	<b>1558</b>	<b>1625</b>
Evapotranspiration		mm	768	602	858	753	746	952	811
		%	49	69	53	48	48	59	88
Runoff		mm	351	73	341	201	320	176	63
		%	23	8	21	13	21	11	7
Infiltration		mm	439	200	427	603	491	497	44
		%	28	23	26	39	32	31	5
<i>Elevation bands project</i>		<b>Precipitation</b>	<b>mm</b>	<b>1845</b>	<b>1372</b>	<b>2292</b>	<b>1904</b>	<b>1885</b>	<b>2188</b>
	Evapotranspiration	mm	435	473	370	285	353	378	309
		%	24	35	16	15	19	17	20
	Runoff	mm	619	226	759	410	599	441	359
		%	34	16	33	22	32	20	24
	Infiltration	mm	791	672	1162	1210	932	1369	860
		%	43	49	51	64	49	63	56

598

599 No field data are available for comparison, but values of water partitioning obtained from the  
600 elevation bands project are more consistent with previous studies over similar snow-dominated  
601 subbasins. Etchevers (2000), using the ISBA-CROCUS model over some snow-dominated  
602 alpine watersheds, found a AET fraction ranging from 24.1% to 35.8%, infiltration from 50%  
603 to 57%, and runoff from 11.5% and 21.3%. Habets et al. (1999) obtained similar result when  
604 studying the Upper Rhône watersheds: an AET of about 25%. Habets et al. (2008), at national

605 scale, find for most part of our catchment, an annual mean ratio of evaporation to precipitation  
606 lower than 0.25.

607 Changes in annual values are mainly due to modification of the snow cover dynamics and  
608 present a great level of disparity depending on seasonality.

609

610 Figure 5 illustrates differences between each project at a monthly time step. Strong seasonal  
611 differences appear: the presences of a spring snow cover on the upper part of the watersheds  
612 influence clearly the ratio between infiltrated and evapotranspired water. In SWAT, when a  
613 snow cover is present, melt water is added to the precipitation and partitioned between only  
614 runoff and infiltration (evaporation is automatically excluded). Sublimation of snow is included  
615 in the AET calculations, but its impact appears limited on the global balance. The decrease in  
616 air temperature that results from the use of elevation bands will also be detrimental to AET over  
617 the year.

618

619 **[Fig5 approximately here]**

620 As suspected, modifications in the upper part of the subbasins change the hydrological  
621 behaviour from upstream to downstream. As discussed in Section 3.1, a better representation  
622 of the snow related processes have allowed simulation improvements. For instance, Figure 6  
623 details the hydrograph for each gauging station and project.

624

625 **[Fig6 approximately here]**

626 As suggested by the improvement in performance, hydrographs from the elevation band project  
627 provide a better fit to the observed values, mainly for high flows in spring and summer -  
628 excluding Auterive gauging station which flows are underestimated in all three projects. The  
629 reference project produces high flow peak that are well synchronised with the observations but

630 that underestimates them notably. The snow parameters project most of the time performs better  
631 in term of magnitude but not in terms of synchronicity.

632

633 Low flows are not improved by introducing elevation bands. Dessens and Bücher (1997)  
634 highlighted that the Pyreneans precipitation lapse rate varies seasonally: it was found twice  
635 more important in winter than in summer. Introduction of a yearly homogenous lapse rate, as  
636 in SWAT, may thus lead to hydrological modelling errors.

637

638

639

## 640 **5. Conclusion**

641

642 Comparison of three calibration projects revealed that the implementation of elevation bands  
643 and their associated altitudinal lapse rates had a positive impact on the hydrological simulation  
644 of the Upper Garonne watershed. Without elevation bands, the identification of snow-related  
645 parameters alone failed to improve the reference project notably. In fact, it turned out somehow  
646 detrimental, producing gains at some sites but losses at others. The positive impact of the  
647 elevation bands cascaded downstream (large improvement at Portlet), which is extremely  
648 positive for the modelling of the whole watershed. In accordance with Zhang et al. (2008), this  
649 conclusion emphasises the importance of spatially detailed snow computation.

650

651 The accuracy of SWAT snow simulations was compared with MODIS and snowpack depth  
652 data. The former confirmed the reasonably good quality of the SWAT spatial representation of  
653 the snow presence, despite the lack of reservoir management data insofar as those reservoirs  
654 are mostly used for low flow support. However, SWAT also slightly overestimated the snow

655 cover at the end of snow season and delays the snow water equivalent peak and the end of the  
656 snowmelt. Comparison with the snow depth time series revealed that SWAT overestimates  
657 snow water content in higher elevations and underestimates it in lower ones. Overestimation of  
658 snow in term of extent and timing at the end of the snowmelt is directly related to the  
659 overestimation of snow water content in the upper elevation bands.

660 Increases in annual precipitation induced by a linear and yearly homogenous precipitation lapse  
661 rate calibrated over the overall watershed revealed the limits of SWAT dealing with the spatial  
662 (nonlinearity in terms of elevation) and temporal variabilities (variation over the year).  
663 Inclusion of lapse rates influenced the water partitioning in snow-dominated subbasins. The  
664 runoff and infiltration increase across affected subbasins, when evapotranspiration decreases  
665 under the effect of a snow cover. Water budget computed by the elevation band project turned  
666 out more in accordance with similar findings on other catchments. Stream flows are also  
667 improved by elevation bands. Simulated high discharge peaks, supported by a larger  
668 groundwater contribution and a more persistent snow cover, are time-shifted and their  
669 amplitude extended.

670 The importance of snow simulation processes and associated parameters has been highlighted.  
671 Even though snow-dominated areas represented just a portion of the catchment, it is beneficial  
672 to use elevation bands. This enhancement echoes the ability of SWAT in representing the snow  
673 cover. It is recommended to eventually compare the two available definitions of elevation bands  
674 in SWAT: area and elevation. This subject will need to be explored in further studies in order  
675 to test the difference between each option in regard to snow simulation. Beyond those  
676 considerations and the reasonably good representation of the snow accumulation and melt  
677 obtained in this study, there are still place for further improvements. For instance, lapse rates  
678 computations remain problematic because of their spatiotemporal variability. Snow  
679 representation could probably be improved if each snow-dominated subbasin could be

680 calibrated individually with a dedicated gauging station and weather station. One may also  
681 consider a lapse rate that varies seasonally.

682

### 683 ***Acknowledgements***

684 Authors acknowledge the financial support given by the Natural Sciences and Engineering Research Council of  
685 Canada and the Institut Hydro-Québec en environnement, développement et société. Simon Gascoin was supported  
686 by the Pyrenees Climate Change Observatory (OPCC-POCTEFA EFA 235/11). Collaboration with Simon  
687 Gascoin was part of the **REGARD** project (Modélisation des ressources en eau sur le bassin de la **Garonne**:  
688 interaction entre les composantes naturelles et anthropiques et apport de la télédétection) - RTRA Sciences et  
689 Technologies pour l'Aéronautique et l'Espace - 2014-2017.

690 We sincerely thank Météo-France for meteorological data and AEAG for hydrological discharge data providing

691

692

693 References

- 694
- 695 Abbaspour, K.C., 2013. SWAT-CUP 2012 : SWAT Calibration and Uncertainty Programs -  
696 A User Manual. , 103 pp.
- 697 Abbaspour, K.C., Johnson, C.A., van Genuchten, M.T., 2004. Estimating uncertain flow and  
698 transport parameters using a sequential uncertainty fitting procedure. *Vadose Zone*  
699 *Journal*, 3(4): 1340-1352.
- 700 Arnold, J.G., Allen, P.M., Bernhardt, G., 1993. A Comprehensive Surface-Groundwater Flow  
701 Model. *Journal of Hydrology*, 142(1-4): 47-69.
- 702 Arnold, J.G. et al., 2012. Swat: Model Use, Calibration, and Validation. *Transactions of the*  
703 *Asabe*, 55(4): 1491-1508.
- 704 ASTER, 2011. Global Digital Elevation Model V2 90x90m. In: NASA(LPDAAC), METI  
705 (Eds.).
- 706 Barnett, T.P., Adam, J.C., Lettenmaier, D.P., 2005. Potential impacts of a warming climate on  
707 water availability in snow-dominated regions. *Nature*, 438(7066): 303-309.
- 708 Bieger, K., Hörmann, G., Fohrer, N., 2014. Simulation of Streamflow and Sediment with the  
709 Soil and Water Assessment Tool in a Data Scarce Catchment in the Three Gorges  
710 Region, China. *J. Environ. Qual.*, 43(1): 37-45.
- 711 Boithias, 2012. Modélisation des transferts de pesticides à l'échelle des bassins versants en  
712 période de crue Université Paul Sabatier Toulouse.
- 713 Boithias, L. et al., 2011. Occurrence of metolachlor and trifluralin losses in the Save river  
714 agricultural catchment during floods. *J Hazard Mater*, 196: 210-219.
- 715 Caballero, Y. et al., 2007. Hydrological sensitivity of the Adour-Garonne river basin to  
716 climate change. *Water Resources Research*, 43(7).
- 717 Castellani, 1986. Régionalisation des précipitations annuelles par la méthode de la régression  
718 linéaire simple : l'exemple des Alpes du Nord. *Revue de géographie alpine*: 393-403.
- 719 Chea, R., 2012. Modélisation des transferts d'eau et des matière en suspension dans un  
720 continuum fluvial lors des événements extrêmes, Toulouse.
- 721 CLC, 2006. Corine Land Cover In: EuropeanUnion(EEA) (Ed.).
- 722 Coughlan, J., Running, S., 1997. Regional ecosystem simulation: A general model for  
723 simulating snow accumulation and melt in mountainous terrain. *Landscape Ecology*,  
724 12(3): 119-136.
- 725 DeBeer, C.M., Pomeroy, J.W., 2009. Modelling snow melt and snowcover depletion in a  
726 small alpine cirque, Canadian Rocky Mountains. *Hydrological Processes*, 23(18):  
727 2584-2599.
- 728 Dessens, J., Bücher, A., 1997. A Critical Examination of the Precipitation Records at the Pic  
729 Du Midi Observatory, Pyrenees, France. In: Diaz, H., Beniston, M., Bradley, R.  
730 (Eds.), *Climatic Change at High Elevation Sites*. Springer Netherlands, pp. 113-121.
- 731 Douglas-Mankin, K.R., Srinivasan, R., Arnold, J.G., 2010. Soil and Water Assessment Tool  
732 (SWAT) model: Current developments and applications. *Trans. Asabe*, 53(5): 1423-  
733 1431.
- 734 Douville, H. et al., 2002. Sensitivity of the hydrological cycle to increasing amounts of  
735 greenhouse gases and aerosols. *Clim Dynam*, 20(1): 45-68.
- 736 Dupeyrat, A., Agosta, C., Sauquet, E., Hendrickx, F., 2008. Sensibilité aux variations  
737 climatiques d'un bassin à fort enjeux - Cas de la Garonne, 13th IWRA world water  
738 congress, Montpellier, France.
- 739 Dwyer, J., Schmidt, G., 2006. The MODIS Reprojection Tool. In: Qu, J., Gao, W., Kafatos,  
740 M., Murphy, R., Salomonson, V. (Eds.), *Earth Science Satellite Remote Sensing*.  
741 Springer Berlin Heidelberg, pp. 162-177.
- 742 ESDB, 2006. european soil data base v2.0, 1kmx1km "dominant value and dominant STU"  
743 Rasters In: (EEA), E.u. (Ed.).

- 744 Etchevers, P., 2000. Modélisation du cycle continental de l'eau à l'échelle régionale. Impact de  
745 la modélisation de la neige sur l'hydrologie du Rhône, Toulouse III.
- 746 Fassnacht, S.R., Heun, C.M., Latrón, J., López Moreno, J.I., 2010. Variability of snow density  
747 measurements in the Río Esera Valley, Pyrenees Mountains, Spain. *Cuadernos de*  
748 *Investigación Geográfica*, 36(1): 59-72.
- 749 Ferrant, S. et al., 2011. Understanding nitrogen transfer dynamics in a small agricultural  
750 catchment: Comparison of a distributed (TNT2) and a semi distributed (SWAT)  
751 modeling approaches. *Journal of Hydrology*, 406(1-2): 1-15.
- 752 Fischer, J., 1932. Le régime de la Garonne pyrénéenne. *Revue géographique des Pyrénées et*  
753 *du Sud-Ouest*: 281-354.
- 754 Fontaine, T.A., Cruickshank, T.S., Arnold, J.G., Hotchkiss, R.H., 2002. Development of a  
755 snowfall–snowmelt routine for mountainous terrain for the soil water assessment tool  
756 (SWAT). *Journal of Hydrology*, 262(1–4): 209-223.
- 757 Garen, D.C., Marks, D., 1996. spatially distributed snow modelling in mountainous regions:  
758 boise river application. In: N°235, I.P. (Ed.), *HydroGIS 96: application of geographic*  
759 *information systems in hydrology and water resources management.*, Vienna.
- 760 Gascoin, S. et al., 2015. A snow cover climatology for the Pyrenees from MODIS snow  
761 products. *Hydrol. Earth Syst. Sci.*, in press(11): 12531-12571.
- 762 Gassman, P.W., Reyes, M.R., Green, C.H., Arnold, J.G., 2007. The soil and water assessment  
763 tool: Historical development, applications, and future research directions. *Trans.*  
764 *Asabe*, 50(4).
- 765 Gassman, P.W., Sadeghi, A.M., Srinivasan, R., 2014. Applications of the SWAT Model  
766 Special Section: Overview and Insights. *J. Environ. Qual.*, 43(1): 1-8.
- 767 Gurtz, J., Lang, H., Verbunt, M., Zappa, M., 2005. The Use of Hydrological Models for the  
768 Simulation of Climate Change Impacts on Mountain Hydrology. In: Huber, U.,  
769 Bugmann, H.M., Reasoner, M. (Eds.), *Global Change and Mountain Regions.*  
770 *Advances in Global Change Research.* Springer Netherlands, pp. 343-354.
- 771 Habets, F. et al., 2008. The SAFRAN-ISBA-MODCOU hydrometeorological model applied  
772 over France. *J. Geophys.Res.*, 113(D06113).
- 773 Habets, F. et al., 1999. Simulation of the water budget and the river flows of the Rhone basin.  
774 *Journal of Geophysical Research: Atmospheres*, 104(D24): 31145-31172.
- 775 Hall, D.K., Riggs, G.A., 2007. Accuracy assessment of the MODIS snow products.  
776 *Hydrological Processes*, 21(12): 1534-1547.
- 777 Hall, D.K., Salomonson, V.V., Riggs, G.A., 2006. MODIS/Terra Snow Cover 8-Day L3  
778 Global 500m Grid, Version 5. In: oulder, C.U.N.S.a.I.D.C. (Ed.).
- 779 Hendrickx, F., Sauquet, E., 2013. Impact of warming climate on water management for the  
780 Ariège River basin (France). *Hydrological Sciences Journal*, 58(5): 976-993.
- 781 Hong, W., Park, M., Park, J., Park, G., Kim, S., 2010. The spatial and temporal correlation  
782 analysis between MODIS NDVI and SWAT predicted soil moisture during forest  
783 NDVI increasing and decreasing periods. *KSCE J Civ Eng*, 14(6): 931-939.
- 784 Kirchner, M. et al., 2013. Altitudinal temperature lapse rates in an Alpine valley: trends and  
785 the influence of season and weather patterns. *Int J Climatol*, 33(3): 539-555.
- 786 Klein, A.G., Barnett, A.C., 2003. Validation of daily MODIS snow cover maps of the Upper  
787 Rio Grande River Basin for the 2000–2001 snow year. *Remote Sens Environ*, 86(2):  
788 162-176.
- 789 Lopez-Moreno, J.I. et al., 2013. Small scale spatial variability of snow density and depth over  
790 complex alpine terrain: Implications for estimating snow water equivalent. *Adv Water*  
791 *Resour*, 55: 40-52.
- 792 Luo, Y., Arnold, J., Allen, P., Chen, X., 2012. Baseflow simulation using SWAT model in an  
793 inland river basin in Tianshan Mountains, Northwest China. *Hydrol. Earth Syst. Sci.*,  
794 16(4): 1259-1267.

795 Magand, C., Ducharne, A., Le Moine, N., Gascoin, S., 2013. Introducing Hysteresis in Snow  
796 Depletion Curves to Improve the Water Budget of a Land Surface Model in an Alpine  
797 Catchment. *Journal of Hydrometeorology*, 15(2): 631-649.

798 Martelloni, G., Segoni, S., Lagomarsino, D., Fanti, R., Catani, F., 2012. Snow Accumulation-  
799 Melting Model (SAMM) for integrated use in regional scale landslide early warning  
800 systems. *Hydrol. Earth Syst. Sci. Discuss.*, 9(8): 9391-9423.

801 McKay, M.D., Beckman, R.J., Conover, W.J., 1979. A Comparison of Three Methods for  
802 Selecting Values of Input Variables in the Analysis of Output from a Computer Code.  
803 *Technometrics*, 21(2): 239-245.

804 Minder, J.R., Mote, P.W., Lundquist, J.D., 2010. Surface temperature lapse rates over  
805 complex terrain: Lessons from the Cascade Mountains. *Journal of Geophysical  
806 Research: Atmospheres*, 115(D14): D14122.

807 Nash, J.E., Sutcliffe, J.V., 1970. River flow forecasting through conceptual models part I — A  
808 discussion of principles. *Journal of Hydrology*, 10(03): 282-290.

809 Neitsch, S.L., Arnold, J.G., Kiniry, J.R., Williams, J.R., 2011. Soil and Water Assessment  
810 Tool - Theoretical Documentation - version 2009.

811 Oeurng, C., Sauvage, S., Sanchez-Perez, J.M., 2011. Assessment of hydrology, sediment and  
812 particulate organic carbon yield in a large agricultural catchment using the SWAT  
813 model. *Journal of Hydrology*, 401(3-4): 145-153.

814 Ouyang, W., Hao, F., Skidmore, A.K., Toxopeus, A.G., 2010. Soil erosion and sediment yield  
815 and their relationships with vegetation cover in upper stream of the Yellow River. *Sci  
816 Total Environ*, 409(2): 396-403.

817 Pagès, M., Miró, J.R., 2010. Determining temperature lapse rates over mountain slopes using  
818 vertically weighted regression: a case study from the Pyrenees. *Meteorological  
819 Applications*, 17(1): 53-63.

820 Palazón, L., Navas, A., 2014. Modeling sediment sources and yields in a Pyrenean catchment  
821 draining to a large reservoir (Ésera River, Ebro Basin). *Journal of Soils and  
822 Sediments*, 14(9): 1612-1625.

823 Parajka, J., Blöschl, G., 2008. Spatio-temporal combination of MODIS images – potential for  
824 snow cover mapping. *Water Resources Research*, 44(3): W03406.

825 Pardé, M., 1936. Le régime de la Garonne. *Revue de géographie alpine*: 254-258.

826 Park, M., Ha, R., Kim, N., Lim, K., Kim, S., 2013. Assessment of future climate and  
827 vegetation canopy change impacts on hydrological behavior of Chungju dam  
828 watershed using SWAT model. *KSCE J Civ Eng*: 1-12.

829 Pepin, N., Kidd, D., 2006. Spatial temperature variation in the Eastern Pyrenees. *Weather*,  
830 61(11): 300-310.

831 Pinglot, F., 2012. Mountainous river stream flow modeling via ArcSWAT: a challenge,  
832 Toulouse.

833 Pradhanang, S.M. et al., 2011. Application of SWAT model to assess snowpack development  
834 and streamflow in the Cannonsville watershed, New York, USA. *Hydrological  
835 Processes*, 25(21): 3268-3277.

836 Probst, J.L., 1983. Hydrologie du bassin de la Garonne : Modèles de Mélange, Bilan de  
837 l'Erosion, Exportation des Nitrates et des Phosphates, Univ. Toulouse.

838 Rahman, K. et al., 2013. Streamflow Modeling in a Highly Managed Mountainous Glacier  
839 Watershed Using SWAT: The Upper Rhone River Watershed Case in Switzerland.  
840 *Water Resour Manag*, 27(2): 323-339.

841 Rijckborst, H., 1967. Hydrology of the Upper-Garonne Basin, Valle de Arán, Spain. J. J.  
842 Groen & Zoon.

843 Sauquet, E. et al., 2010. IMAGINE 2030, climat et aménagements de la Garonne : quelles  
844 incertitudes sur la ressource en eau en 2030? (IMAGINE 2030, climate and water

845 management: uncertainties on water resources for the Garonne river basin in 2030?),  
846 IRSTEA.

847 Stehr, A., Debels, P., Arumi, J.L., Romero, F., Alcajaga, H., 2009. Combining the Soil and  
848 Water Assessment Tool (SWAT) and MODIS imagery to estimate monthly flows in a  
849 data-scarce Chilean Andean basin. *Hydrological Sciences Journal*, 54(6): 1053-1067.

850 Stratton, B.T., Sridhar, V., Gribb, M.M., McNamara, J.P., Narasimhan, B., 2009. Modeling  
851 the Spatially Varying Water Balance Processes in a Semiarid Mountainous Watershed  
852 of Idaho1. *JAWRA Journal of the American Water Resources Association*, 45(6):  
853 1390-1408.

854 Strauch, M., Volk, M., 2013. SWAT plant growth modification for improved modeling of  
855 perennial vegetation in the tropics. *Ecol Model*, 269(0): 98-112.

856 Troin, M., Caya, D., 2014. Evaluating the SWAT's snow hydrology over a Northern Quebec  
857 watershed. *Hydrological Processes*, 28(4): 1858-1873.

858 Verbunt, M. et al., 2003. The hydrological role of snow and glaciers in alpine river basins and  
859 their distributed modeling. *Journal of Hydrology*, 282(1-4): 36-55.

860 Viviroli, D. et al., 2011. Climate change and mountain water resources: overview and  
861 recommendations for research, management and policy. *Hydrol. Earth Syst. Sci.*,  
862 15(2): 471-504.

863 Viviroli, D., Weingartner, R., 1999. The hydrological significance of mountains: from  
864 regional to global scale. *Hydrol. Earth Syst. Sci.*, 8(6): 1017-1030.

865 Viviroli, D., Weingartner, R., Messerli, B., 2003. Assessing the Hydrological Significance of  
866 the World's Mountains. *Mt Res Dev*, 23(1): 32-40.

867 Voirin-Morel, S., 2003. Modélisation distribuée des flux d'eau et d'énergie et des débits à  
868 l'échelle régionale du bassin Adour-Garonne, Uni. Toulouse III.

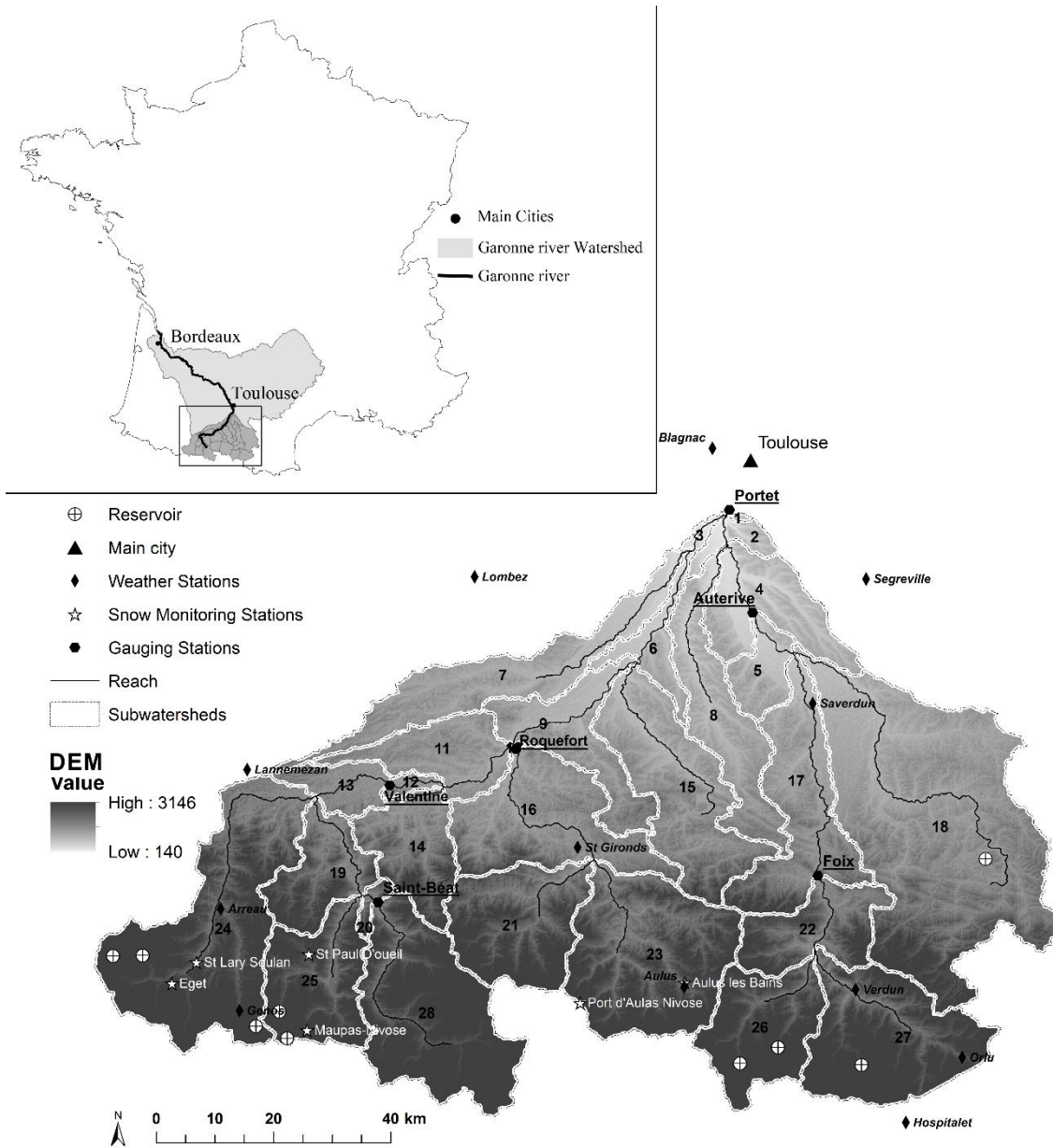
869 Wang, X., Melesse, A.M., 2005. Evaluation of the SWAT model's snowmelt hydrology in a  
870 northwestern Minnesota watershed *Transactions of the ASAE* 48(4): 1359-1376

871 Yang, J., Reichert, P., Abbaspour, K.C., Xia, J., Yang, H., 2008. Comparing uncertainty  
872 analysis techniques for a SWAT application to the Chaohe Basin in China. *Journal of*  
873 *Hydrology*, 358(1-2): 1-23.

874 Zeinivand, H., Smedt, F., 2009. Hydrological Modeling of Snow Accumulation and Melting  
875 on River Basin Scale. *Water Resour Manag*, 23(11): 2271-2287.

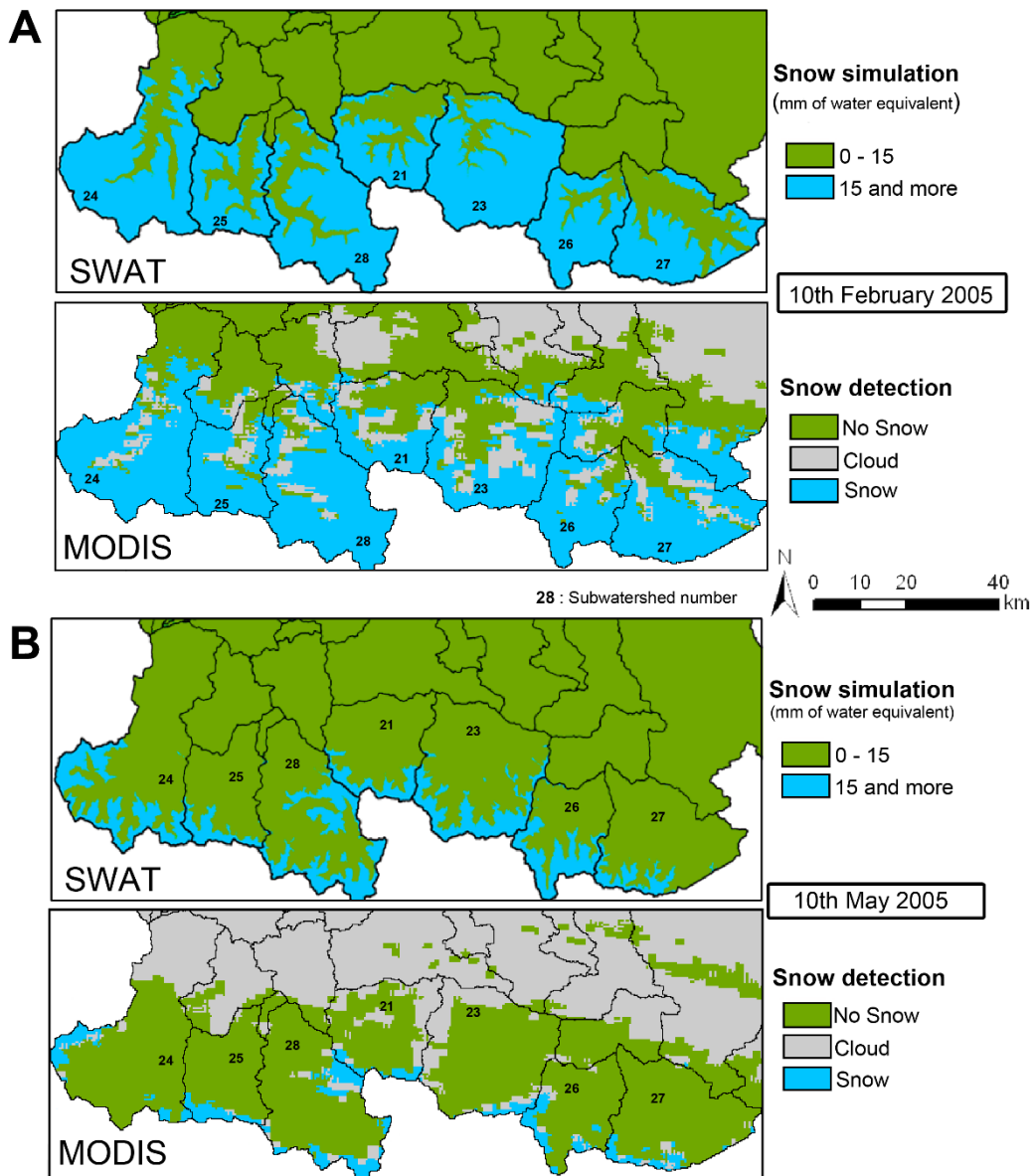
876 Zhang, X., Srinivasan, R., Debele, B., Hao, F., 2008. Runoff Simulation of the Headwaters of  
877 the Yellow River Using The SWAT Model With Three Snowmelt Algorithms.  
878 *JAWRA Journal of the American Water Resources Association*, 44(1): 48-61.

879  
880



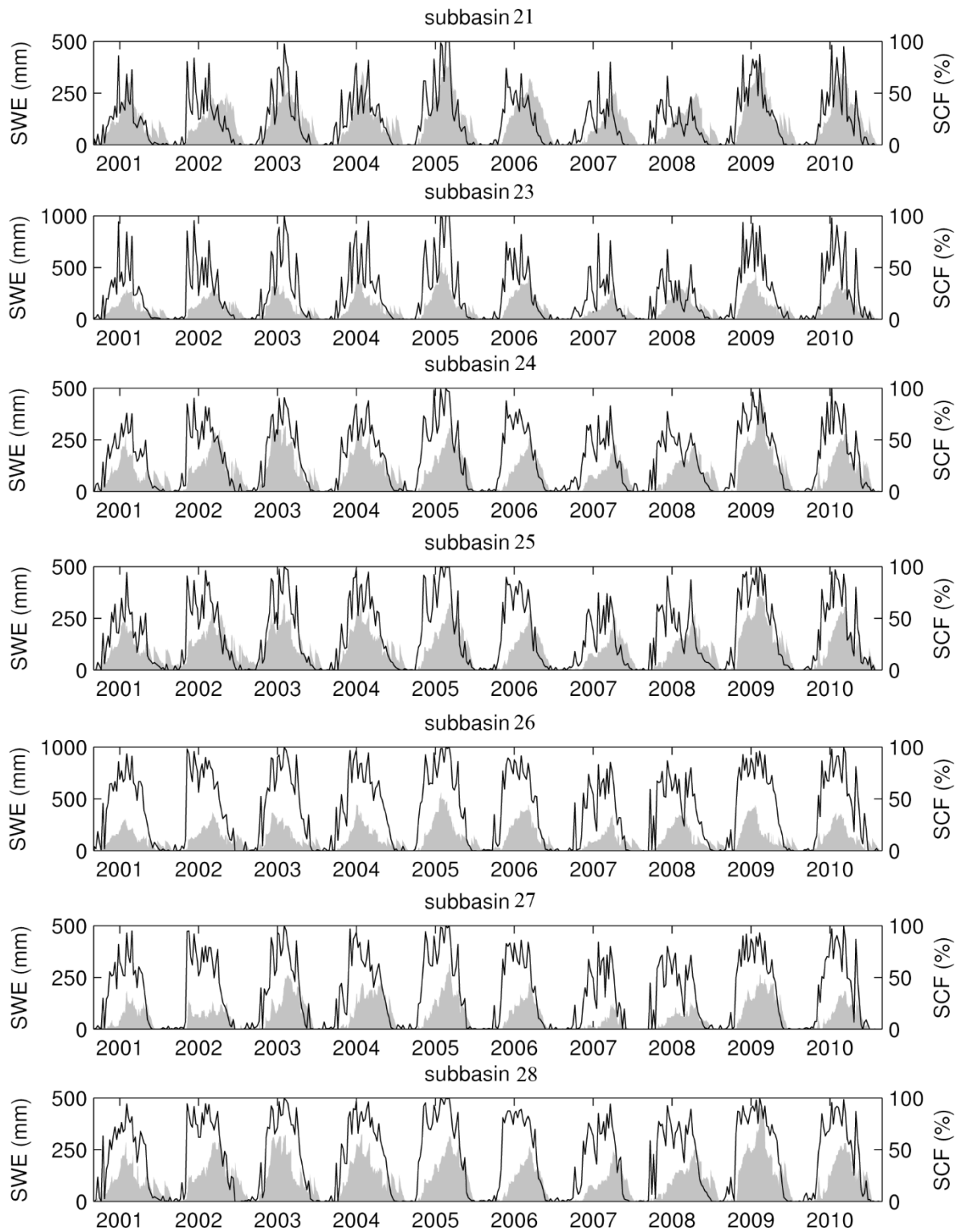
881  
882  
883

Figure 1: Geographic situation of the headwater Garonne watershed.



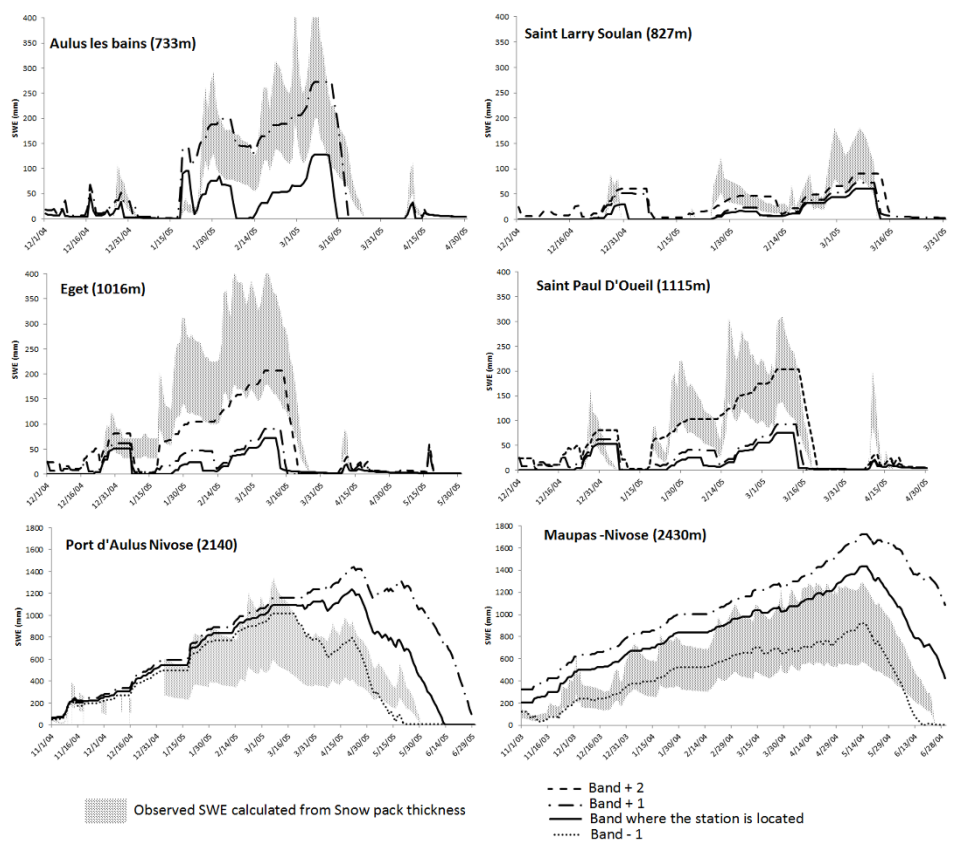
884  
885  
886  
887

**Figure 2: Snow comparison: A) 10 February 2005 B) 10 May 2005**



888  
 889  
 890  
 891  
 892

**Figure 3: Temporal snow comparison.** Solid black line represents the daily percentage of snow cover detected by MODIS at subbasin scale, while the grey surface is SWAT snow water equivalent



893  
894  
895  
896  
897

**Figure 4: Snow water equivalent comparison between SWAT and a range of possible values calculated from observations**

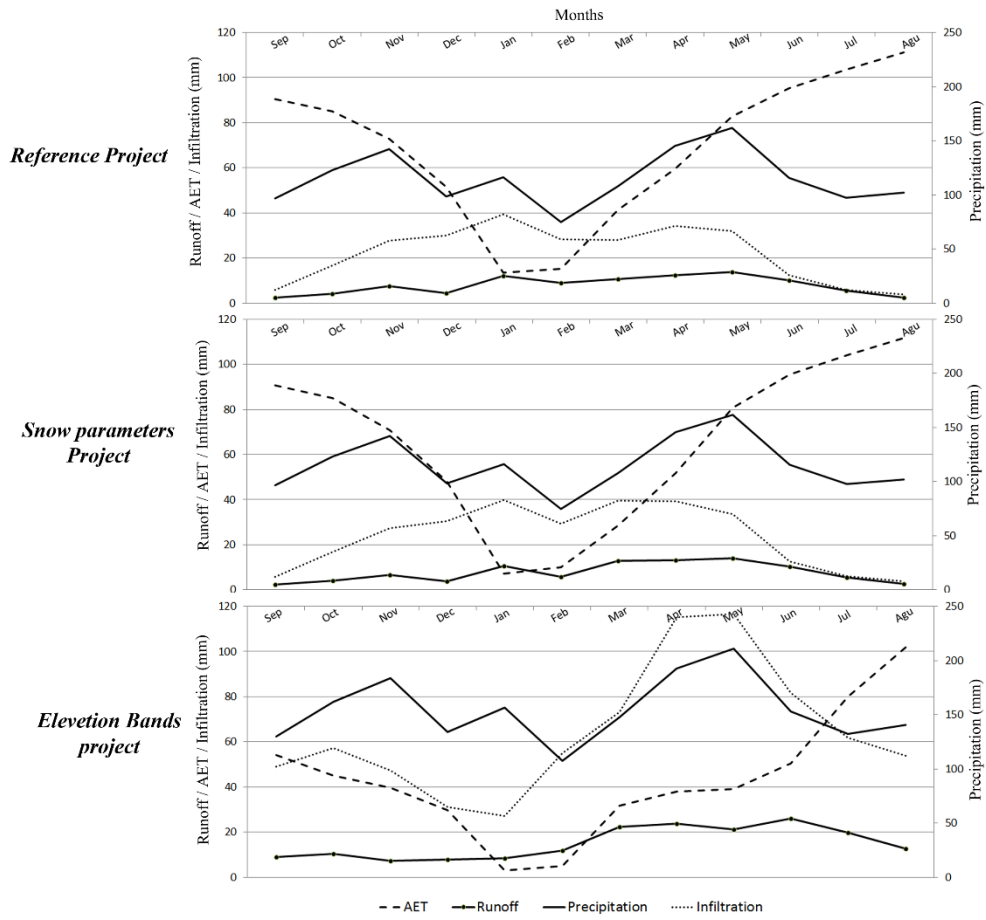
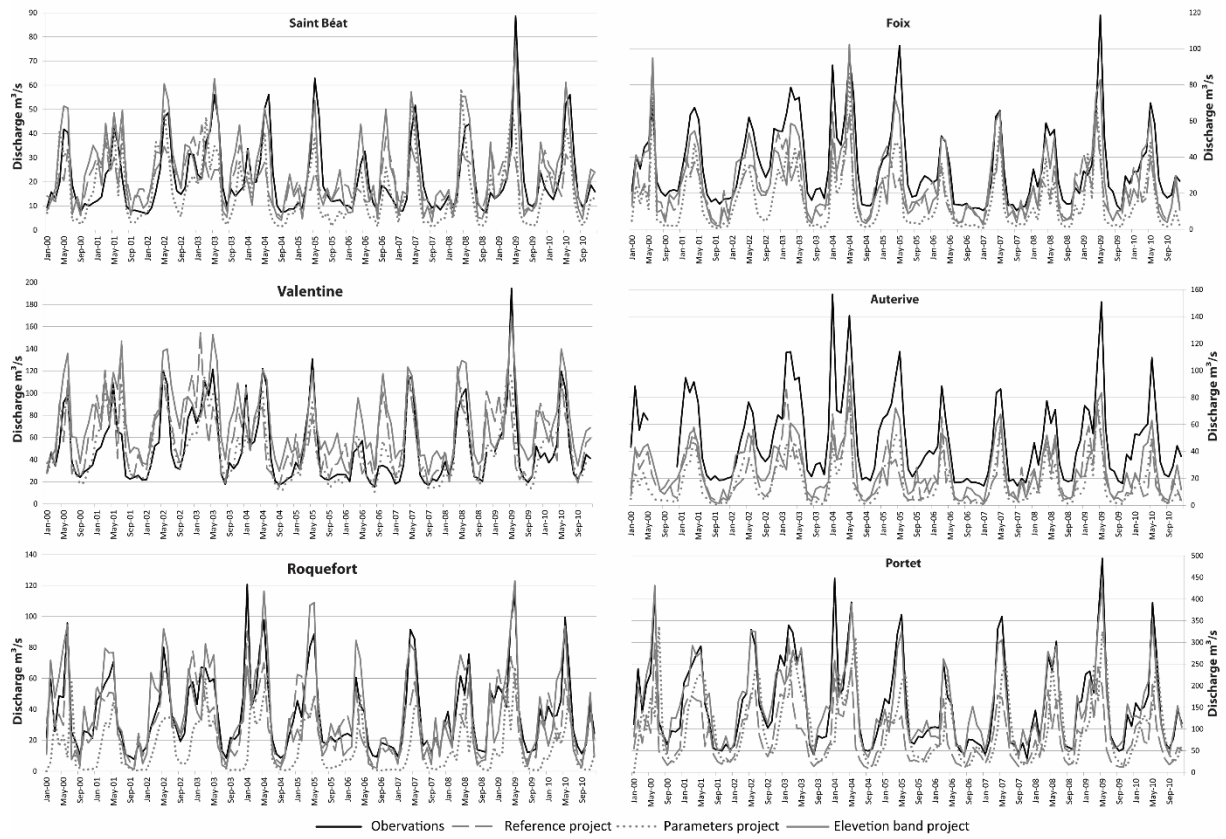


Figure 5: Monthly mean values of snow dominated subwatersheds over 2000-2010

898  
899  
900  
901



902  
903  
904  
905

Figure 6: Hydrographs for the 6 gauging stations